Molecular Therapy
Nucleic Acids
Original Article

miR-539-5p regulates *Srebf1* transcription in the skeletal muscle of diabetic mice by targeting DNA methyltransferase 3b

Devesh Kesharwani,[1,2] Amit Kumar,[1,2] Ashima Rizvi,[1,2] and Malabika Datta[1,2]

[1]CSIR-Institute of Genomics and Integrative Biology, Mall Road, Delhi 110007, India; [2]Academy of Scientific and Innovative Research, CSIR-HRDC, Kamala Nehru Nagar, Ghaziabad, Uttar Pradesh 201002, India

Aberrant DNA methylation is associated with diabetes, but the precise regulatory events that control the levels and activity of DNA methyltransferases (DNMTs) is not well understood. Here we show that miR-539-5p targets *Dnmt3b* and regulates its cellular levels. miR-539-5p and *Dnmt3b* show inverse patterns of expression in skeletal muscle of diabetic mice. By binding to the 3′ UTR of *Dnmt3b*, miR-539-5p downregulates its levels in C2C12 cells and in human primary skeletal muscle cells. miR-539-5p-*Dnmt3b* interaction regulates *Srebf1* transcription by altering methylation at CpG islands within *Srebf1* in C2C12 cells. *Dnmt3b* inhibition alone was sufficient to upregulate *Srebf1* transcription. *In vivo* antagonism of miR-539-5p in normal mice induced hyperglycemia and hyperinsulinemia and impaired oral glucose tolerance. These mice had elevated *Dnmt3b* and decreased *Srebf1* levels in skeletal muscle. db/db mice injected with miR-539-5p mimics showed improved circulatory glucose and cholesterol levels. Oral glucose tolerance improved together with normalization of *Dnmt3b and Srebf1* levels in skeletal muscle. Our results support a critical role of miR-539-5p and *Dnmt3b* in aberrant skeletal muscle metabolism during diabetes by regulating *Srebf1* transcription; modulating the miR-539-5p-*Dnmt3b* axis might have therapeutic potential for addressing altered skeletal muscle physiology during insulin resistance and type 2 diabetes.

INTRODUCTION

Type 2 diabetes is a highly complex metabolic disease marked by insulin resistance and/or impaired insulin secretion. A strong genetic association is implicated in the manifestation of diabetes,[1] but most of these incompletely explain the high discordance among monozygotic twins and close correlations with environmental factors.[2,3] Therefore, non-genetic factors, primarily epigenetic modifications, gradually gained acceptance as critical contributing causal factors of the onset and progression of diabetes. An epigenome association study has reported alterations in DNA methylation patterns to be closely linked to whole-body insulin sensitivity.[4]

DNA methyltransferases (DNMTs) catalyze the reversible covalent transfer of a methyl group to the C-5 position of a cytosine residue in the DNA, usually present in stretches of CpG islands.[5] In mammals, DNMTs encompass a family of five members: DNMT1, DNMT2, DNMT3a, DNMT3b, and DNMT3L. However, only DNMT1, DNMT3a, and DNMT3b demonstrate DNA methyl transfer activity. Although DNMT1 is involved in the replication process, DNMT3a and DNMT3b are *de novo* DNMTs and are implicated in establishing new DNA methylation patterns. Such patterns undergo dynamic and reversible remodeling that determines transcript levels of various genes during different cellular processes that consequently govern cell fate and function.[6,7] Therefore, regulatory events that determine the levels and function of DNMTs are important for maintenance of normal cellular physiology.

As with other genes, DNMTs are also regulated at transcriptional, translational, and post- translational levels. At the transcriptional level, DNMTs are regulated by several transcription factors, such as Sp1, Sp3, p53, Rb, Foxo3a, etc. The promoters of DNMT3a and DNMT3b contain multiple binding sites for several transcription factors; Sp1 acts as transcriptional activator, and Sp3 acts as an activator or a repressor of Sp1-mediated transcription.[8] In a colon carcinoma cell line, HCT116, p53 negatively regulates DNMT1 expression by forming a complex with Sp1.[9] The promoters of DNMT1 and DNMT3a also harbor binding sites for E2F, and the Rb protein inhibits DNMT expression by binding with E2F and consequently promoting global hypomethylation.[10] DNMT3b expression is negatively regulated by Foxo3a by interacting with specific binding sites on the DNMT3b promoter.[11]

Several reports suggest that DNMTs are also regulated by post-translational modifications. Cellular levels and activities of DNMT1 and DNMT3a have been shown to be influenced by post-translational modifications like phosphorylation, methylation, and SUMOylation. Although SUMOylation of DNMT3a modifies its ability to interact with other proteins ,[12] lysine methylation of

Received 20 October 2021; accepted 10 August 2022;
https://doi.org/10.1016/j.omtn.2022.08.013.

Correspondence: Malabika Datta, CSIR-Institute of Genomics and Integrative Biology, Mall Road, 110007 Delhi, India.
E-mail: mdatta@igib.res.in

DNMT1 affects its stability and signals for its proteasomal degradation.[13,14] The cellular activity and genome methylation patterns are determined by serine phosphorylation of DNMTs.[14,15] It is believed that an interplay between the various regulatory post-translational modifications of DNMTs determines their stability and activity. The RNA binding protein HuR has been shown to post-transcriptionally regulate DNMT3b by binding to its 3′ UTR and increasing its levels in colorectal cancer cells, affecting DNMT3b-specific target DNA methylation.[16]

In addition, microRNAs (miRNAs) have, in the recent past, been identified as major regulators of DNMTs. Particularly members of the miR-29 family have been reported to directly target DNMT3a and DNMT3b and affect global DNA methylation.[17,18] miR-29b targets and downregulates Sp1, a major transcriptional regulator of DNMT1, and indirectly regulates its levels.[18] miR-148 targets DNMT3b[19] and DNMT1[20] and promotes DNA hypomethylation of methylation-sensitive genes. DNMT1 has been reported to be targeted by miR-126 and miR-152 by specific binding at the 3′ UTR, resulting in silencing of crucial methylation-sensitive tumor suppressor genes.[20,21]

Despite these regulatory features of DNMT modulation, not much is known about such events in skeletal muscle during diabetes. This is significant because it is known that DNMT levels and activity are increased in skeletal muscle and subsequently modify the methylome, as seen in this tissue during diabetes.[22–25]

In this study, we present data to demonstrate the regulation of DNMT3b by miR-539-5p and the resulting consequences of this event for impaired skeletal muscle physiology during diabetes.

RESULTS

DNMT and miRNA expression is altered in skeletal muscle of db/db mice

Several studies have shown altered patterns of DNA methylation in skeletal muscle during diabetes.[22–25] In this study, we sought to evaluate whether miRNAs might regulate the expression of DNMTs and consequently regulate DNA methylation patterns. In a previous study from our laboratory, we had shown that, compared with normal db/+ mice, there exists an altered miRNA signature in skeletal muscle of diabetic db/db mice.[26] To interrogate whether these altered miRNAs might target DNMTs in skeletal muscle, we used online tools that predict miRNA-target-interacting sites (TargetScan, miRanda, and miRDB). Although *Dnmt3b* was predicted to be targeted by three downregulated miRNAs, miR-539-5p, miR-381-3p, and miR-31-5p, *Dnmt3a* was a potential target of miR-374, miR-455, and miR-883a-3p. None of the altered miRNAs were predicted to target *Dnmt1*. We therefore began this study by evaluating the status of *Dnmt3a* and *Dnmt3b* in skeletal muscle of diabetic mice. Although transcript and protein levels of *Dnmt3b* were significantly elevated in skeletal muscle of diabetic mice, those of DNMT3a were unchanged (Figures 1A–1D). Concomitantly, compared with normal mice, DNMT activity was significantly increased in skeletal muscle of diabetic mice (Figure 1E). Although *Dnmt1* was not predicted to be targeted by any of the altered miRNAs as stated above, we desired to assess the levels of DNMT1 in skeletal muscle of normal and diabetic mice. As shown in Figure 1F, compared with normal db/+ mice, DNMT1 levels were significantly decreased in skeletal muscle of diabetic mice. Because DNMT activity is increased (Figure 1E) in skeletal muscles of diabetic db/db mice, we think this is the result of increased DNMT3b levels. Because DNMT3b levels were increased and also predicted to be targeted by the downregulated miRNAs, we probed the status of the miRNAs that were predicted to target *Dnmt3b* and therefore, might be responsible for the observed changes in DNMT3b levels (Figures 1B and 1D). TargetScan, miRDB, and miRanda revealed *Dnmt3b* to be targeted by the downregulated miRNAs miR-539-5p, miR-381-3p, and miR-31-5p. The expression of these three miRNAs was validated in skeletal muscle of db/db mice. As in the microarray profiling in a previous study,[26] compared with normal mice, the levels of all the three miRNAs were significantly downregulated in the skeletal muscle during diabetes (Figures 1G–1I). Such inverse patterns of expression between *Dnmt3b* and these three miRNAs indicate that *Dnmt3b* levels might be regulated by these miRNAs during diabetes.

miR-539-5p targets *Dnmt3b* by binding to its 3′ UTR

To validate the above, C2C12 cells were transfected with varied doses of miRNA mimics (1–50 nM) corresponding to miR-539-5p, miR-381-3p, and miR-31-5p, and the levels of DNMT3b were evaluated by western blot analysis. There was a significant dose-dependent decrease in expression of DNMT3b in the presence of miR-539-5p (Figure 2A). However, there was no significant change in expression of DNMT3b with overexpression of miR-381-3p or miR-31-5p in C2C12 cells (Figure 2A). The miR-539-5p mimic-mediated (50 nM) decrease in DNMT3b levels was significantly prevented in the presence of the miR-539-5p inhibitor (Figures 2B and 2C) at the transcript and protein level, suggesting a specific effect of miR-539-5p on DNMT3b. Overexpression of miR-539-5p mimics at a dose of 50 nM caused an almost 500-fold increase over its endogenous levels (~60,000 copies/cell) (data not shown). To validate direct binding of miR-539-5p on *Dnmt3b*, we generated luciferase reporter constructs of the wild-type 3′ UTR (wild type [WT]) of *Dnmt3b* harboring the miR-539-5p binding site (Figure 2D) and also a mutated construct (MT) with a swap of 4 nt within the seed region of miR-539-5p binding site (Figure 2D). C2C12 cells were co-transfected with the WT or the MT 3′ UTR reporter plasmid along with the miR-539-5p mimic with or without the miR-539-5p inhibitor. There was a significant decrease in the luciferase activity of the WT construct in the presence of miR-539-5p, and this was significantly prevented in the presence of miR-539-5p inhibitor and with the construct harboring a mutation in the miR-539-5p binding site (Figure 2E), suggesting that miR-539-5p binds to the 3′ UTR of *Dnmt3b*. This was confirmed using a biotin-labeled miR-539-5p mimic. C2C12 cells were transfected with biotin-labeled scramble or biotin-labeled miR-539-5p, and after 48 h, cells transfected with biotin-labeled miR-539-5p mimics demonstrated binding of the miRNA mimic to the *Dnmt3b* 3′ UTR, as evident by significant enrichment of the

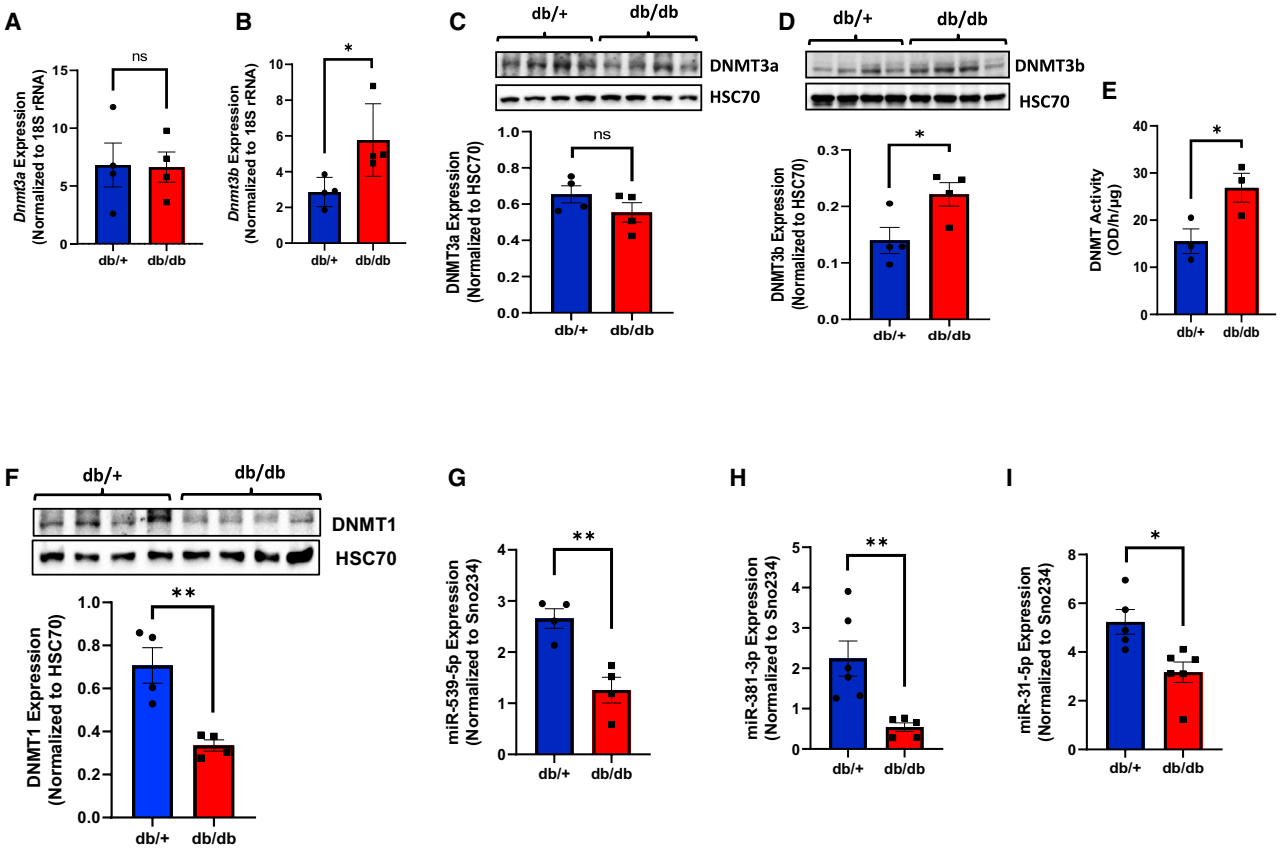

Figure 1. Expression of DNMTs and miRNAs is altered in skeletal muscle of db/db mice

(A and B) Total RNA was isolated from the skeletal muscles of normal (db/+) and diabetic (db/db) mice, and 1 µg RNA was reverse transcribed and subjected to qRT-PCR to assess the transcript levels of *Dnmt3a* (A) and *Dnmt3b* (B). 18S rRNA was used as the loading control. (C and D) Skeletal muscle of normal (db/+) and diabetic (db/db) mice was lysed as described under "Materials and methods;" 40-µg lysates were run on SDS-PAGE, and the levels of DNMT3a (C) and DNMT3b (D) were evaluated by western blot analysis. HSC70 was used as a loading control. Densitometric analyses of the expression are shown below. (E) Skeletal muscle of normal (db/+) and diabetic (db/db) mice was lysed as described under "Materials and methods," and 20-µg lysates were used to measure DNMT activity. (F) DNMT1 protein levels were assessed in skeletal muscle of db/+ and db/db mice by western blot analyses, where 40 µg protein was resolved on SDS-PAGE and probed with a DNMT1 antibody. HSC70 was used as the loading control. Densitometric analyses of the expression are shown below. (G–I) Total RNA was isolated from skeletal muscle of normal (db/+) and diabetic (db/db) mice, and 1 µg RNA was reverse transcribed and subjected to qRT-PCR for expression of miR-539-5p (G), miR-381-3p (H), and miR-31-5p (I). All experiments were performed in at least four animals in each group, and values are reported as means ± SEM. *$p < 0.05$, **$p < 0.01$.

Dnmt3b transcript in the streptavidin pull-down complex (Figure 2F). All of this suggests that miR-539-5p targets *Dnmt3b* and inhibits its expression by binding to its 3′ UTR.

Such a miR-539-5p and *Dnmt3b* interaction was validated in primary human skeletal muscle cells, where miR-539-5p significantly inhibited expression of DNMT3b, and this inhibition was prevented in the presence of a miR-539-5p inhibitor (Figure 2G). The inverse pattern of expression between miR-539-5p and *Dnmt3b* in db/db mice (Figure 1) was validated in a high-fat diet (HFD) model of obesity and diabetes. Compared with chow-diet fed mice, although expression of miR-539-5p was significantly downregulated (Figure 2H), *Dnmt3b* transcript levels were significantly upregulated (Figure 2I) in skeletal muscle of HFD-fed mice. This suggests that miR-539-5p levels are downregulated in skeletal muscle during obesity and diabetes and that, by targeting *Dnmt3b*, this miRNA might be responsible for the deregulated skeletal muscle physiology in these states.

miR-539-5p targets *Dnmt3b* and regulates *Srebf1* levels in C2C12 cells

Because DNMT activity and DNMT3b levels are upregulated in skeletal muscle during diabetes, and this would likely hypermethylate and promote gene silencing, to assess the cellular relevance, we looked for consequent effects on a set of downregulated genes in skeletal muscle of db/db mice taken from a recent study from our laboratory.[27] Pathway enrichment analysis (using DAVID Pathway Analysis 6.8) of the downregulated genes revealed pathways of AMPK and insulin signaling to be significantly overrepresented.[27] Both of these pathways are critical in skeletal muscle metabolism, and three common

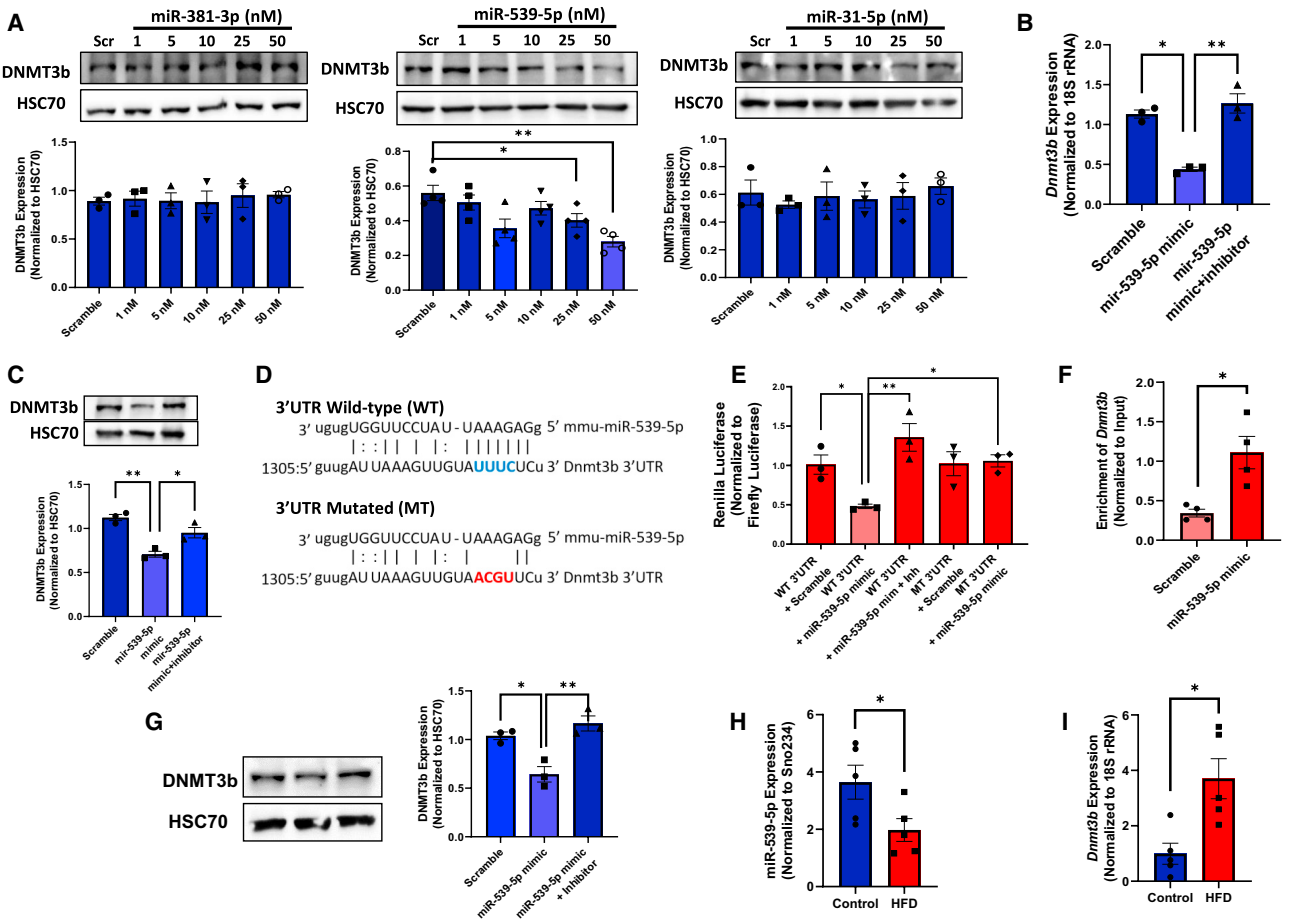

Figure 2. miR-539-5p inhibits *Dnmt3b* levels by binding to its 3′ UTR

(A) Differentiated C2C12 cells were transfected with the scramble (Scr) or mimics of miR-539-5p, miR-381-3p, or miR-31-5p (1–50 nM). Upon termination of incubation at 48 h, cells were lysed, and 40 μg protein was subjected to western blot analysis using a DNMT3b antibody. HSC70 was used as a loading control. Densitometric analyses of the blots are shown below. (B) Differentiated C2C12 cells were transfected with the Scr or the miR-539-5p mimic with or without its inhibitor. After 48 h, transcript levels of *Dnmt3b* were quantified by qRT-PCR. 18S rRNA was taken as the loading control. (C) Cells incubated as in (B) were lysed, and lysates (40 μg) were assessed for DNMT3b protein levels by western blot analysis using a DNMT3b antibody. HSC70 was used as a loading control. Densitometric analysis of the blots is shown below. (D) Depiction of the miR-539-5p binding site in the 3′ UTR of *Dnmt3b* and the mutations (red) incorporated in the miRNA binding site of the *Dnmt3b* 3′ UTR (MT) as described under "Materials and methods." (E) C2C12 cells were transfected with wild-type (WT) or mutated (MT) 3′ UTR luciferase constructs of *Dnmt3b* together with the Scr or the miR-539-5p mimic with or without its inhibitor. After 48 h of incubation, cells were harvested, and luciferase activity was measured as described under "Materials and methods.". *Renilla* luciferase activity was normalized to firefly luciferase activity. (F) C2C12 cells were transfected with biotin-labeled Scr or biotin-labeled miR-539-5p mimic (50 nM), and after 48 h, cells were harvested, lysed, and pulled down using streptavidin-linked Dynabeads. Enrichment of *Dnmt3b* mRNA in biotin-labeled Scr- or miR-539-5p mimic-transfected cells was quantified by real-time PCR using *Dnmt3b*-specific primers. (G) Primary human skeletal muscle cells were transfected with the Scr or the miR-539-5p mimic with or without its inhibitor. Upon termination of incubation (48 h), DNMT3b expression was assessed by western blot analysis using a DNMT3b antibody. HSC70 was used as a loading control. Densitometric analysis of the same is given alongside the blot. All experiments were performed in at least 3 sets for each group. (H and I) 1 μg RNA from skeletal muscle of chow diet- and HFD-fed mice (n = 5) was reverse transcribed and subjected to qRT-PCR to evaluate the expression of miR-539-5p (H) and *Dnmt3b* (I). Sno234 and 18S rRNA, respectively, were used as normalization controls. Values are means ± SEM. *p < 0.05, **p < 0.01.

genes, *Prkab2*, *Srebf1*, and *Irs1* (Figure 3A), from these pathways are significantly downregulated in skeletal muscles of db/db mice, as revealed by RNA sequencing.[27] The expression of these genes in skeletal muscles of db/+ and db/db mice was validated by qRT-PCR, and, as in the RNA sequencing data,[27] these genes were significantly downregulated in db/db mice skeletal muscle (Figure 3B). We hypothesized that this downregulation might be mediated by increased DNMT3b levels, and to investigate this, we examined the presence of CpG islands within these genes. All three genes, *Prkab2*, *Srebf1*, and *Irs1*, harbored varied lengths of CpG islands across their gene lengths (Figure 3C), indicating a possibility of them being regulated by DNA methylation.

For validation, C2C12 cells were transfected with the scramble or miR-539-5p mimic with or without its inhibitor for 48 h. There

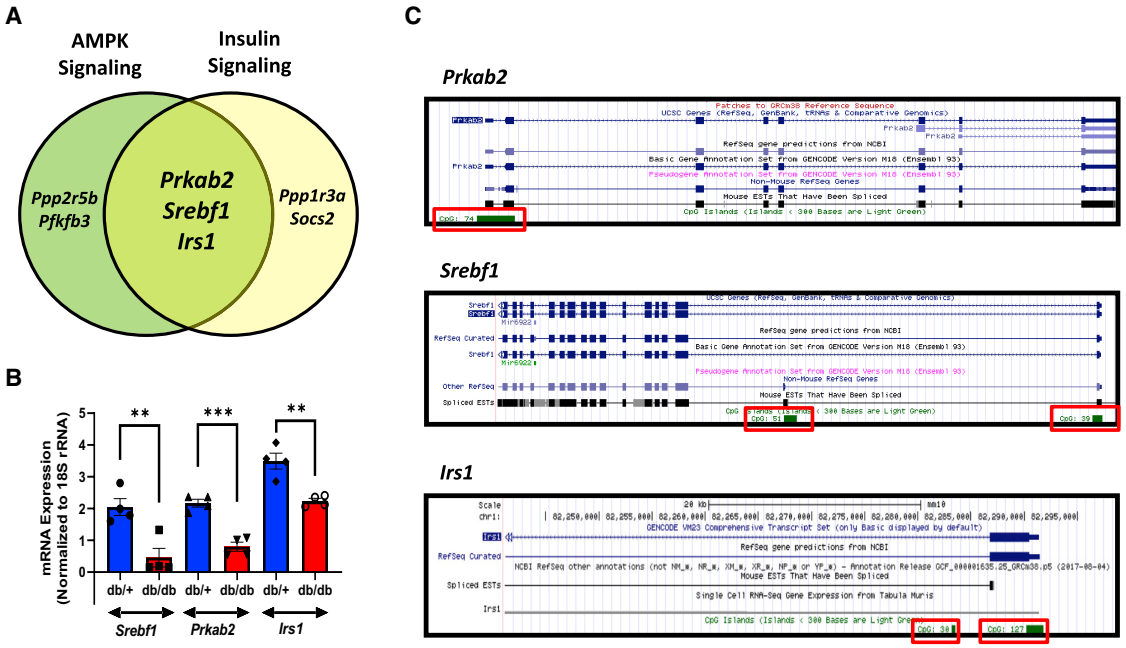

Figure 3. *Srebf1*, *Irs1*, and *Prkab2* harbor CpG islands, and their transcript levels are downregulated in skeletal muscle of db/db mice

(A) AMPK and insulin signaling pathways are enriched among the downregulated genes in db/db mouse skeletal muscle, with *Prkab2*, *Srebf1*, and *Irs1* commonly mapped to both pathways. (B) Skeletal muscle RNA (1 μg) from db/+ and db/db mice was reverse transcribed and subjected to qRT-PCR for transcript expression of *Prkab2*, *Srebf1*, and *Irs1* using gene-specific primers. 18S rRNA was used as the loading control. Data are from at least four animals in each group, and values are means ± SEM. $^{**}p < 0.01$, $^{***}p < 0.001$. (C) Presence of CpG islands (enclosed within red boxes) across the *Prkab2*, *Srebf1*, and *Irs1* genes as identified using the UCSC Genome Browser.

was no change in the transcript levels of *Prkab2* or *Irs1* in the presence of miR-539-5p. Interestingly, miR-539-5p caused a significant increase in the transcript levels of *Srebf1*, which was prevented in the presence of its inhibitor (Figure 4A), suggesting that, because *Srebf1* harbors CpG islands, presumably by inhibiting DNMT3b levels, miR-539-5p decreases methylation of *Srebf1* and increases its levels. To validate this, C2C12 cells were transfected with the scramble or the miR-539-5p mimic, and the methylation status of *Srebf1* was evaluated by methylated DNA immunoprecipitation (MeDIP). Using the UCSC genome browser, two CpG-rich regions were captured within *Srebf1*: site 1 spanning across the promoter and exon 1 and site 2 within intron 1 (Figure 4B). Compared with scramble-transfected cells, there was a significant decrease in methylation at site 1, but there was no significant change at site 2 (Figure 4C), suggesting a role of this miRNA in regulating *Srebf1* methylation by targeting *Dnmt3b* and, consequently, regulating its levels. This methylation status was also validated *in vivo* in normal (db/+) and diabetic (db/db) mouse skeletal muscle, and, as shown in Figure 4D, there was significant hypermethylation of *Srebf1* in db/db mouse skeletal muscle compared with normal db/+ mice. CpG site 2 also demonstrated significantly increased methylation in db/db mouse skeletal muscle; this is possibly mediated by factors other than miR-539-5p *in vivo*. To investigate whether *Dnmt3b* inhibition alone might affect *Srebf1* levels, C2C12 cells were transfected with *Dnmt3b* small interfering RNA (siRNA), and this caused significant inhibition of DNMT3b levels (Figures 4E and 4F) associated with notable increases in *Srebf1* transcript levels at 100 nM (Figure 4G). This was confirmed using nanaomycin A, a selective DNMT3b inhibitor. As shown in Figures 5A and 5B, compared with control cells, although nanaomycin A (NA) significantly inhibited DNMT3b levels at 10 μM, there was no significant change in the transcript or protein levels of DNMT1 and DNMT3a at any of the doses used. This change in DNMT3b levels was not evident at 1 or 5 μM. In Hep3B cells, similar patterns of NA-induced decreases in DNMT3b protein levels at higher doses have been shown by Lai et al.[28] Interestingly, however, there was a modest but significant decrease in DNMT activity in the presence of 5 μM NA, although this inhibitory effect was more pronounced at 10 μM concentration (Figure 5C). Such NA-induced inhibition of DNMT activity at 5 μM without a change at the transcript or protein level has been shown by Kuck et al.[29] This was consequently accompanied by an increase in the transcript levels of *Srebf1* at 10 μM but not at 5 μM (Figure 5D), even though there was a modest decrease in DNMT activity at 5 μM. This may possibly be due to the fact that the modest decrease in DNMT activity at 5 μM NA is not sufficient to exert effects on *Srebf1* transcription. These results suggest that *Dnmt3b* is a crucial regulator of *Srebf1* and that, by targeting *Dnmt3b*, miR-539-5p regulates cellular *Srebf1* levels. To confirm that the miR-539-5p-*Dnmt3b* axis is

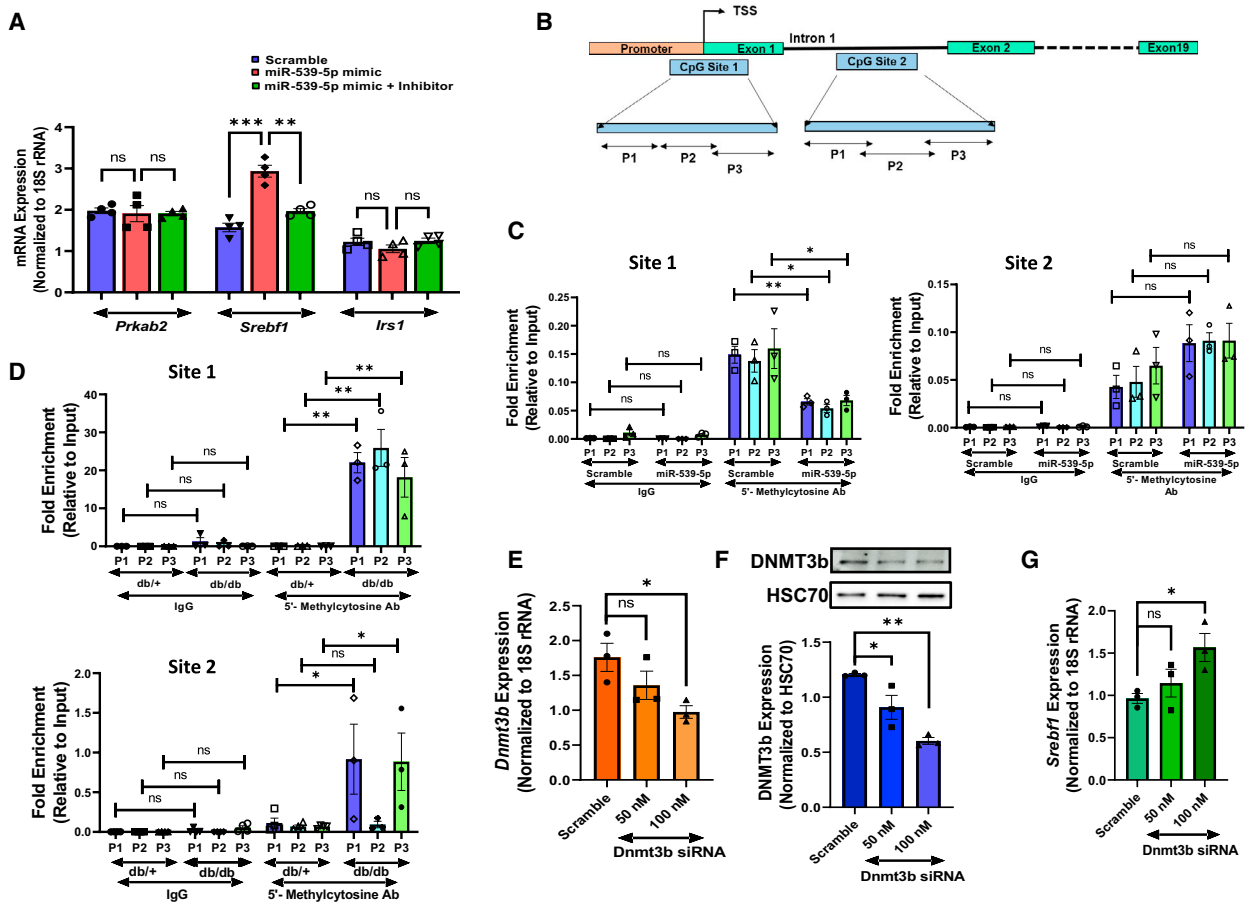

Figure 4. miR-539-5p regulates *Srebf1* transcript levels by inhibiting *Dnmt3b* expression and altering CpG methylation on the *Srebf1* gene in C2C12 cells

(A) Differentiated C2C12 cells were transfected with the Scr or the miR-539-5p mimic with or without its inhibitor. After 48-h incubation, cells were harvested, and expression of transcript levels of *Prkab2*, *Srebf1*, and *Irs1* (as described under "Materials and methods") was evaluated using qRT-PCR. 18S rRNA was used as the loading control. (B) Schematic of CpG islands across the *Srebf1* gene in mice. Each CpG site was randomly split into three regions, and primers were designed to amplify these regions within each CpG island using primers sets (P1, P2, and P3) as shown. (C) Differentiated C2C12 cells were transfected as in (A) with Scr or the miRNA mimic, and upon termination of incubation, genomic DNA was isolated, sheared, and immunoprecipitated (2 μg) with a 5-methylcytosine antibody (2 μg) or non-immune rabbit IgG (2 μg) and incubated overnight at 4°C. Methylation-enriched CpG regions within the *Srebf1* gene were quantified by real-time PCR using CpG region-specific primers. (D) Genomic DNA isolated from skeletal muscle of normal db/+ and diabetic db/db mice was sheared, and the methylation status within *Srebf1* was quantified by real-time PCR as described in (C). Differentiated C2C12 cells were transfected with the Scr or *Dnmt3b* siRNA (50–100 nM), and after 48 h, cells were harvested, and DNMT3b expression was quantified at the transcript (E) and protein (F) levels. 18S rRNA and HSC70 were used as normalization controls, respectively. (G) Differentiated C2C12 cells transfected with the Scr or *Dnmt3b* siRNA (50–100 nM) were harvested, and 1 μg RNA was reverse transcribed to evaluate the transcript levels of *Srebf1* by qRT-PCR. 18S rRNA was used as the normalization control. Values are means±SEM of at least three independent experiments. *p < 0.05, **p < 0.01, ***p < 0.001. ns, non-significant.

important in determining cellular *Srebf1* levels, endogenous miR-539-5p levels in C2C12 cells were inhibited using the miR-539-5p inhibitor, and levels of its target, *Dnmt3b* and *Srebf1* were evaluated. As shown in Figures 5E–G, inhibition of endogenous miR-539-5p led to a significant increase in DNMT3b levels, and this was accompanied by a decrease in the transcript levels of *Srebf1*. To validate whether such decreases in *Srebf1* are due to miR-539-5p inhibitor-mediated increases in *Dnmt3b*, we inhibited *Dnmt3b* levels in the presence of the miR-539-5p inhibitor. *Dnmt3b* levels were inhibited using specific siRNAs, and, as shown in Figures 5H and 5I, inhibiting *Dnmt3b* levels significantly rescued miR-539-5p inhibitor-mediated decrease in *Srebf1* transcript levels. To explore whether *Dnmt3b* overexpression can rescue miR-539-5p effects on *Srebf1* transcription, C2C12 cells were transfected with the empty vector or the *Dnmt3b* overexpression vector (0.5–1 μg). Transfection with the *Dnmt3b* overexpression vector led to an approximately 300- and 700-fold dose-dependent increase in endogenous *Dnmt3b* levels at 0.5- and 1-μg doses, respectively. Subsequently, transfection of C2C12 cells with the miR-539-5p mimic together with the *Dnmt3b* overexpression vector (1 μg) significantly rescued the miR-539-5p-mediated increase in *Srebf1* transcript levels (Figure 5J). This

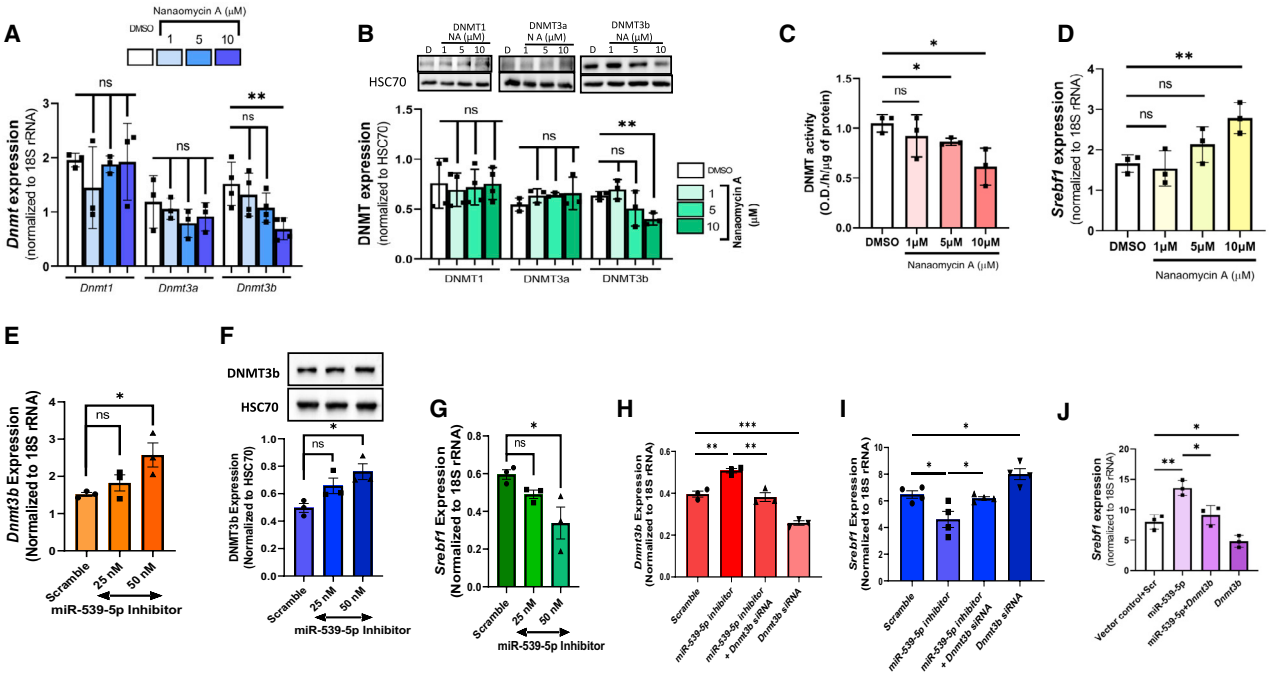

Figure 5. *Dnmt3b* inhibition rescues the miR-539-5p inhibitor-induced decrease in *Srebf1* levels in C2C12 cells

(A and B) C2C12 cells were incubated in the presence of a DNMT3b inhibitor (nanaomycin A [NA]) at doses of 1, 5, and 10 μM. Control cells were incubated in the presence of DMSO. After 48 h, DNMT1, DNMT3a, and DNMT3b levels were evaluated by qRT-PCR (A) and western blot (B). 18S rRNA and HSC70, respectively, were used as the loading controls. D, DMSO. (C) Cells incubated as in (A) were assayed for activity of DNMT as described under "Materials and methods." Data were normalized to the total protein content. (D) Total RNA was isolated from cells incubated as in (A), and the transcript levels of *Srebf1* were quantified using specific primers. 18S rRNA was used as the normalization control. (E–G) C2C12 cells were transfected with the Scr or miR-539-5p inhibitor (25–50 nM), and after 48 h, the status of DNMT3b (E and F) and *Srebf1* (G) were evaluated by qRT-PCR and western blot analysis. HSC70 and 18S rRNA were taken as the normalizing controls for western blot and qRT-PCR experiments, respectively. (H and I) C2C12 cells were transfected with the Scr or miRNA-539-5p alone (50 nM) or along with *Dnmt3b* siRNA (100 nM), and after 48 h, *Dnmt3b* (H) and *Srebf1* (I) transcript levels were evaluated by qRT-PCR. 18S rRNA was taken as the endogenous control. (J) C2C12 cells were transfected with the empty vector or the *Dnmt3b* overexpression vector (1 μg) together with the Scr or miR-539-5p (50 nM); after 48 h, total RNA was isolated, and the transcript levels of *Srebf1* were evaluated by qRT-PCR. 18S rRNA was used as the endogenous control. All experiments were performed at least three times for each group, and values are reported as means ± SEM. *p < 0.05, **p < 0.01, ***p < 0.001.

indicates that the effects of miR-539-5p on *Srebf1* are mediated through DNMT3b.

In vivo antagonism of miR-539-5p induces hyperglycemia and impairs oral glucose tolerance in mice

To determine the physiological significance of the miR-539-5p-*DNMT3b* interaction, mice were injected intravenously (i.v.) with the scramble or the miR-539-5p antagomir at a dose of 5 mg/kg. A schematic of the injection schedule and experimental protocol is shown in Figure 6A. Blood glucose was measured randomly on the next day after every injection, and there was significant increase in blood glucose levels in antagomir-injected mice compared with scramble-injected mice (Figure 6B). After 6 and 12 h of fasting, there was a significant increase in fasting glucose levels in miR-539-5p antagomir-administered mice (Figure 6C) together with increased circulatory insulin levels (Figure 6D). An oral glucose tolerance test (OGTT) demonstrated significant impairment in glucose tolerance in antagomir-injected mice compared with scramble-injected mice (Figure 6E). Compared with scramble-injected mice, serum triglycerides and cholesterol levels were also significantly elevated in miR-539-5p antagomir-injected mice (Figures 6F and 6G). All of these results demonstrate that inhibition of miR-539-5p impairs glucose metabolism and alters serum lipid profiles in mice.

miR-539-5p inhibition *in vivo* alters *DNMT3b* and *Srebf1* expression in skeletal muscle of mice

Because, as shown above, administration of the miR-539-5p antagomir induces hyperglycemia, hyperinsulinemia, and hyperlipidemia in mice, we sought to examine DNMT3b and *Srebf1* levels in skeletal muscle of these mice. miR-539-5p antagomir administration to mice significantly increased DNMT3b levels in skeletal muscle (Figures 7A and 7B) and decreased the transcript levels of *Srebf1* (Figure 7C), indicating that, by increasing DNMT3b levels, miR-539-5p antagonism decreases *Srebf1* transcription in skeletal muscle tissue *in vivo*. However, compared with scramble-injected mice, neither *Dnmt3b* nor *Srebf1* transcript levels were altered in the livers of miR-539-5p antagomir-injected mice (Figures 7D and 7E), indicating

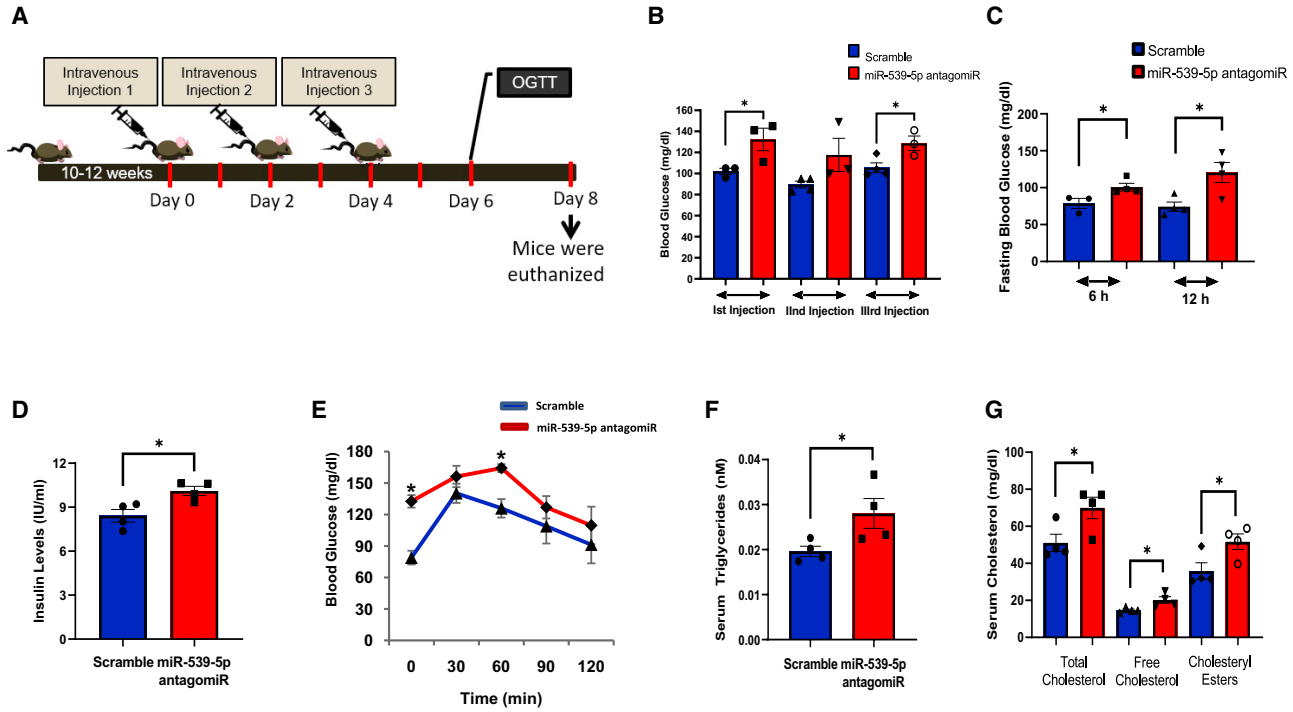

Figure 6. *In vivo* antagonism of miR-539-5p induces hyperglycemia and hyperinsulinemia in mice

(A) Schematic of the *in vivo* experimental pipeline. C57BL/6 mice were injected i.v. with Scr or miR-539-5p antagomir at a dose of 5 mg/kg. Three injections were given, one every other day. An OGTT was done on day 6, and on day 8, mice were euthanized. (B) Blood glucose levels were measured randomly the following day after every injection. (C and D) Fasting blood glucose levels at 6 and 12 h of fasting (C) and circulatory insulin levels (D) were measured in Scr- and miR-539-5p antagomir-injected mice. (E) OGTT was performed on Scr- and miR-539-5p antagomir-injected mice after 12 of fasting. (F and G) Serum triglyceride (F) and cholesterol (G) levels were measured in sera of Scr- and miR-539-5p antagomir-injected mice as described under "Materials and methods." Data are from at least four animals in each group, and values are means ± SEM. *$p < 0.05$ compared with Scr-injected mice.

that the effects of miR-539-5p on *Dnmt3b* and *Srebf1* are possibly tissue specific. This was evident because transfection of hepatic Hepa 1-6 cells with the miR-539-5p (50 nM) mimic did not cause any significant change in the transcript levels of *Dnmt3b* or *Srebf1* (Figure 7F).

In vivo administration of miR-539-5p normalizes hyperglycemia, improves oral glucose tolerance, and restores miR-539-6p, *Dnmt3b*, and *Srebf1* levels in skeletal muscle of db/db mice

A schematic of the *in vivo* protocol is shown in Figure 8A. Random and fasting glucose levels were measured, and after the final injection, an OGTT was done, and skeletal muscle tissues were collected. As shown in Figure 8B, compared with db/db mice injected with the scramble, miR-539-5p-administered mice showed a significant improvement in random blood glucose levels that were measured the next day after each injection. Fasting glucose levels and oral glucose tolerance also significantly improved in miR-539-5p-administered db/db mice compared with scramble-administered db/db mice (Figures 8C and 8D). miR-539-5p significantly improved serum triglyceride and cholesterol levels in db/db mice, although cholesteryl esters remained unchanged (Figures 8E and 8F). Compared with scramble-injected db/db mice, in skeletal muscle of miR-539-5p-administered db/db mice, there was an increase in the levels of miR-539-5p and a concomitant decrease in the levels of *Dnmt3b* (Figures 8G and H). *Srebf1* levels also significantly improved upon miR-539-5p administration to db/db mice (Figure 8I).

DISCUSSION

In this study, we present data to show that miR-539-5p targets DNMT3b and consequently regulates *Srebf1* transcript levels in skeletal muscle during diabetes.

Aberrant DNA methylation is linked to several diseases, including cancers, heart diseases, inflammation, skin diseases, etc.[30–33] DNA methylation mediated by DNMTs is a covalent modification of DNA and almost exclusively occurs at cytosine residues in CpG islands that are frequently located within the promoter regions and close to transcription start sites. Such modifications determine the spatial and temporal patterns of transcript levels within a cell and signify the importance of DNMT regulation in cellular physiology. The activity and cellular levels of DNMTs are regulated at the level of activation, stabilization, and recruitment at specific sites and heterochromatin regions on the

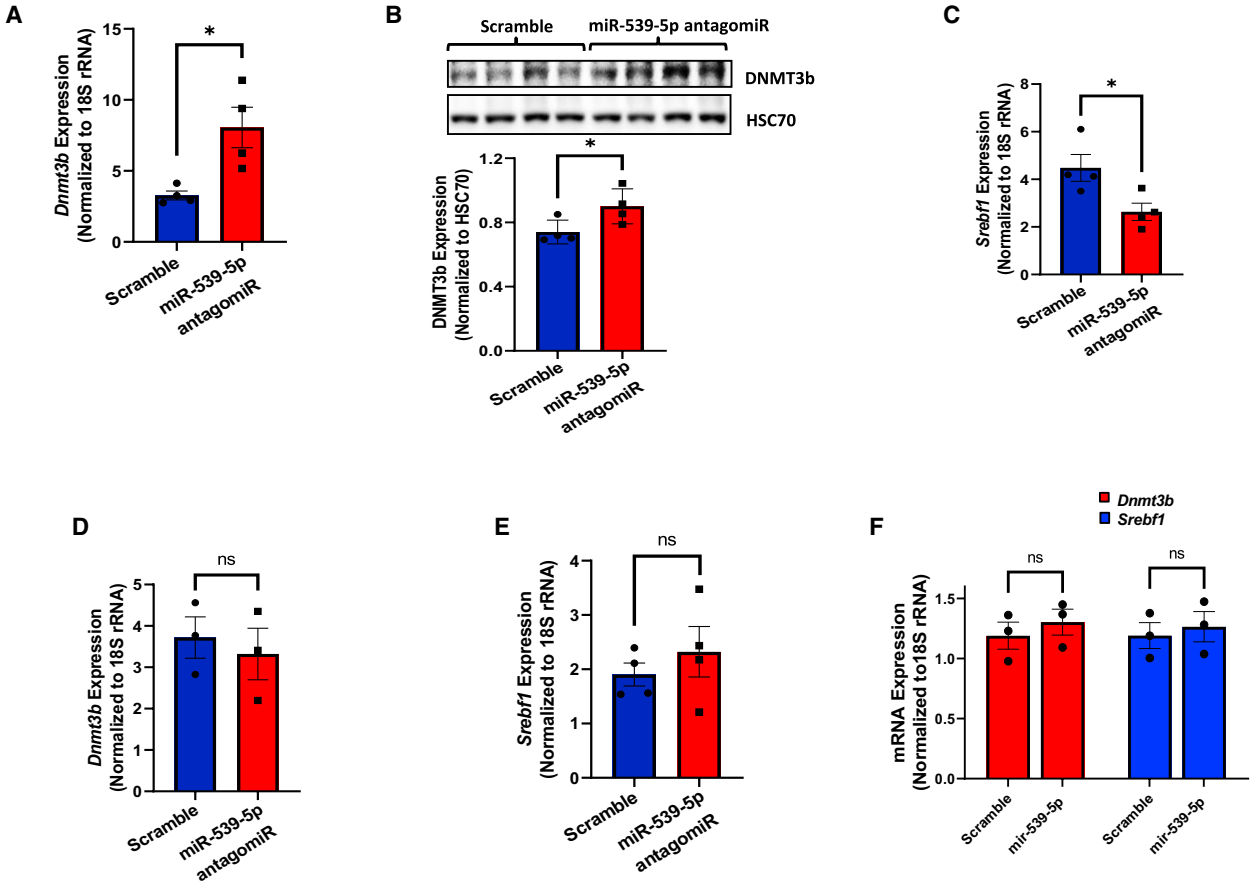

Figure 7. *In vivo* inhibition of miR-539-5p induces DNMT3b expression and inhibits *Srebf1* expression in skeletal muscle

(A) Total RNA (1 μg) isolated from skeletal muscle of Scr- and miR-539-5p antagomir-injected mice was reverse transcribed and assessed for the transcript levels of *Dnmt3b* by qRT-PCR. 18S rRNA was used as endogenous control. (B) Skeletal muscle tissue from Scr- and miR-539-5p antagomir-injected mice was homogenized in lysis buffer, and 40 μg protein was run for SDS-PAGE and subjected to western blot analysis for detection of DNMT3b using specific antibodies. HSC70 was used as a loading control. (C) 1 μg of RNA from skeletal muscle tissue of Scr- and miR-539-5p antagomir-injected mice was reverse transcribed, and transcript levels of *Srebf1* were evaluated by qRT-PCR. 18S rRNA was used as a normalizing control. (D and E) Total RNA (1 μg) from the livers of Scr- and miR-539-5p antagomir-injected mice was reverse transcribed, and transcript levels of *Dnmt3b* (D) and *Srebf1* (E) were evaluated by qRT-PCR. 18S rRNA was used as a normalization control. (F) Mouse hepatic Hepa 1-6 cells were transfected with the Scr or miR-539-5p mimic (50 nM). After 48 h, cells were harvested to evaluate the expression of *Dnmt3b* and *Srebf1* transcripts by qRT-PCR, normalized to 18S rRNA. Data are from at least 4 animals in each group, and data in (F) are from experiments in three independent sets; values are means ± SEM. *$p < 0.05$ compared with Scr-injected mice.

DNA.[34] This may be mediated by transcription factors, piRNA complexes, other noncoding RNAs, and post-translational modifications.[35,36]

In the recent past, miRNAs have been identified as significant regulators of DNMTs. Members of the miR-29 family target DNMT3a and DNMT3b and affect global DNA methylation patterns.[17,18] Other miRNAs, like miR-126, miR-152, and miR-148, have also been shown to directly target and alter levels of DNMTs. Embryonic stem cells from Dicer-deficient mice have significantly decreased levels of DNMT1, DNMT3a, and DNMT3b.[37,38] Our current study demonstrates regulation of DNMT3b by miR-539-5p in skeletal muscle during diabetes. DNMT3b and miR-539-5p display inverse patterns of expression in skeletal muscle of db/db and HFD diabetic mice. By binding to the 3′ UTR of *Dnmt3b*, miR-539-5p significantly decreases the transcript and protein levels of DNMT3b. These data suggest a critical role of miRNAs in mediating post-transcriptional regulation of DNMTs at the onset and during progression of diverse diseased states.

Abnormal DNMT levels trigger aberrant methylation patterns of genes that consequently regulate their expression levels and cell function. Interestingly, DNMT3b, in its dual capacity, controls diverse cellular events. It provides accessory functions by supporting the catalytic activity of other DNMTs, HDACs, etc.; mediates methylation; represses gene expression; and regulates essential pathways.

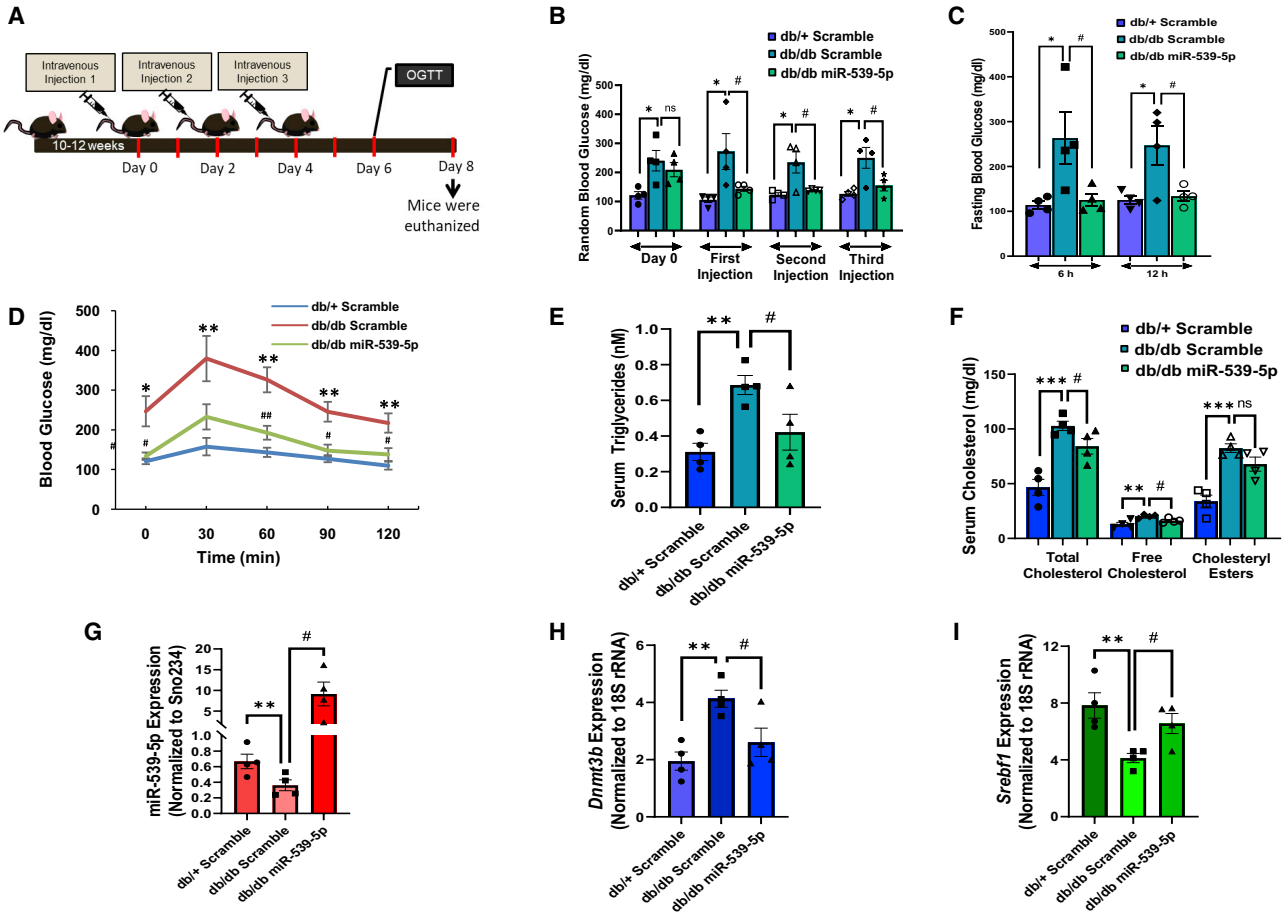

Figure 8. miR-539-5p administration improves hyperglycemia and normalizes miR-539-5p, *Dnmt3b*, and *Srebf1* levels in skeletal muscle of diabetic db/db mice

(A) Schematic of the experimental design for db/+ and db/db animals. db/db mice were injected with the Scr to miR-539-5p mimics (i.v. through the tail vein) at a dose of 5 mg/kg body weight. db/+ mice were injected with Scr. Three injections were given, one every other day. An OGTT was done on day 6, and on day 8, mice were euthanized. (B and C) Random blood glucose levels on the following day after every injection (B) and fasting blood glucose levels at 6 and 12 h of fasting (C) were measured in db/+ and db/db mice. (D) OGTT was performed after an oral glucose dose (2 g/kg body weight), and blood glucose levels were measured at time intervals of 30, 60, 90, and 120 min after the glucose feed. (E and F) Serum triglyceride (E) and cholesterol (F) levels were measured in sera of db/+ and db/db mice. (G–I) Total RNA was isolated from skeletal muscle tissue of db/+ mice injected with the Scr or db/db mice injected with the Scr or miR-539-5p mimics, and the transcript levels of miR-539-5p (G), *Dnmt3b* (H), and *Srebf1* (I) were assessed by qRT-PCR. Sno234 or 18S rRNA was taken as the normalization control. Values are means ± SEM of four animals in each group. *p < 0.05, **p < 0.01, ***p < 0.001 compared with db/+ mice injected with Scr; #p < 0.05, ##p < 0.01 compared with db/db mice injected with Scr.

On the other hand, its intrinsic catalytic function alone at least in part determines its methyltransferase activity, which is evident by hypomethylation of target gene loci in *Dnmt3b*$^{-/-}$ and *Dnmt3b*$^{CI/CI}$ mice (expressing catalytically inactive *Dnmt3b*) compared with WT mice.[39] Generally, hypermethylation of DNA regions close to transcription start sites is associated with suppression of gene expression and vice versa.[5] It is believed that the transcriptional decrease because DNA hypermethylation is possibly due to decreased binding of transcription factors to their respective binding sites. Our study shows that miR-539-5p, by inhibiting DNMT3b levels, increases the transcript levels of *Srebf1*. *Srebf1* harbors potential CpG islands at two regions, and the one spanning the transcription start site is hypomethylated in the presence of miR-539-5p, and this elevates *Srebf1* transcription. Although our data support the fact that such hypomethylation is due to a miR-539-5p-targeted decrease in DNMT3b levels and, consequently, of its activity, a contribution of its independent methyltransferase catalytic activity alone cannot be ruled out and needs further investigation, especially because, despite being dispensable, the catalytic activity of DNMT3b is critically associated with genomic elements that control tumorigenesis in mice by regulating processes involved in cellular transformation, including that of phosphatidylinositol 3-kinase (PI3K)-Akt, mitogen-activated kinase (MAPK), etc.[40]

Srebf1 encodes a helix-loop-helix leucine zipper transcription factor, SREBP1, that binds to the sterol regulatory element primarily found

in genes involved in cholesterol biosynthesis and lipid homeostasis. The encoded protein is located at the endoplasmic reticulum and, upon cleavage, translocates to the nucleus to initiate target gene transcription. The *Srebf1* gene is expressed in various tissues,[41,42] and abnormal levels are linked to several diseases, like diabetes, obesity, NAFLD, Parkinson's disease, and hepatocellular carcinoma.[43–46]

With respect to insulin resistance and type 2 diabetes, genetic variability within the *Srebf1* gene is suggested to play a significant role. Genome-wide studies in the European population depict a strong link of type 2 diabetes with the *Srebf1* locus,[47] and single-nucleotide polymorphisms within this gene have been associated with obesity, insulin resistance, and abnormal lipid levels.[46,48,49] *Irs2* gene transcription is repressed by increased hepatic levels of this protein, which impairs insulin sensitivity and promotes hepatic triglyceride accumulation and fatty liver.[50] Hepatic levels of the *Srebf1*-encoded protein SREBP1c are regulated by nutrient stimuli such as glucose and polyunsaturated fatty acids.[51] Insulin upregulates SREBP1c levels in skeletal muscle, which increases the levels of glycolytic and lipogenic genes.[52] A recent study from our laboratory demonstrated decreased transcript levels of *Srebf1* in skeletal muscle of diabetic mice.[27] *Srebf1* transcript levels have been shown to be downregulated in skeletal muscle of diabetic subjects,[53] and, interestingly, these diabetic subjects had poor metabolic control and a negative correlation between *Srebf1* transcript levels and circulatory HbA1c levels.

Our results in the current study show that, by targeting *Dnmt3b*, miR-539-5p increases *Srebf1* transcript levels in skeletal muscle cells. *In vivo* antagonism of miR-539-5p increases DNMT3b levels and downregulates the transcript levels of *Srebf1*. This was accompanied by hyperglycemia, hyperinsulinemia, hypercholesterolemia, and hypertriglyceridemia. Hence, decreased *Srebf1* levels as seen in skeletal muscle during diabetes[27] are due to the increased levels and activity of DNMT3b and the consequent hypermethylation and silencing of *Srebf1*, all triggered by decreased miR-539-5p levels. Our data show that, within skeletal muscles of db/db mice, there is significant hypermethylation at these regions compared with normal db/+ mice. Similar hypermethylation patterns on the *Srebf1* promoter have been reported in the liver and adipose tissue of diabetic subjects.[54] However, in our study, compared with scramble-injected mice, transcript levels of *Srebf1* were not altered in the livers of miR-539-5p antagomir-injected mice. This might be due to the fact that miRNAs are known to exert tissue-specific effects, and miR-539-5p probably does not specifically affect the *Dnmt-3b-Srebf1* axis in the liver. Our data also demonstrate that *in vivo* administration of miR-539-5p to diabetic db/db mice normalizes hyperglycemia and improves oral glucose tolerance together with normalization of *Dnmt3b* and *Srebf1* levels in the skeletal muscle.

This study identifies miR-539-5p as a novel regulator of *Srebf1* transcription and provides key information for modulating its levels for therapeutic intervention. We provide evidence showing that, in skeletal muscle during diabetes, miR-539-5p levels are downregulated, accompanied by increased *Dnmt3b* and decreased *Srebf1* levels. As in the liver and adipose tissue, *Srebf1*-encoded SREBP1c in skeletal muscle mediates insulin effects on specific genes, and its regulation of glycolytic and lipogenic genes indicates its relevance in maintaining muscle insulin sensitivity.[52] These events could be important in aberrant skeletal muscle metabolism in pathophysiological states such as obesity and diabetes.

MATERIALS AND METHODS

Animal experiments

Ten- to twelve-week-old male normal mice (C57BLKs $lep^{db/+}$; body weight, 23.06 ± 0.47 g; blood glucose, 104.5 ± 2.19 mg/dL) and diabetic mice (C57BLKs $lep^{db/db}$; body weight, 42.04 ± 2.19 g; blood glucose, 390.25 ± 57.85 mg/dL) (n = 4) were obtained from the animal house facility of the CSIR-Central Drug Research Institute (CDRI) (Lucknow, India) and maintained with *ad libitum* food and water at the animal house facility of the CSIR-Institute of Genomics and Integrative Biology (IGIB) (Delhi, India). Seven-week-old C57BL/6 male mice obtained from the animal house facility of the CSIR-IGIB were fed a chow diet (10% calories from fat) or HFD (60% calories from fat) (Research Diets, NJ, USA) for 6 months; there was an approximately 40% increase in body weight, and glucose levels increased by around 45% in HFD-fed animals compared with chow diet-fed mice. Mice were euthanized, and skeletal muscle was isolated and stored in RNAlater (Ambion, TX, USA) or transferred to −80°C for further experiments. Another set of 10- to 12-week-old male C57BL/6 mice procured from the animal house facility of the CSIR-IGIB were randomly assigned to two groups (n = 5 per group) and maintained at a 12:12 h light:dark cycle with *ad libitum* food and water. Animals were injected i.v. (three injections, one every other day) with the scramble or miR-539-5p antagomir (Dharmacon, CO, USA) at a dose of 5 mg/kg body weight using *in vivo*-jetPEI (Polyplus-Transfection, France) according to the manufacturer's instructions. Blood glucose of mice was measured randomly the next day after every injection. The day after the third injection, animals were fasted overnight for an OGTT. On the eighth day after the first injection, mice were euthanized, and blood samples and skeletal muscle and liver tissue were collected for further experiments. For *in vivo* injections in normal db/+ mice (C57BLKs; body weight, 24.66 ± 0.76 g; blood glucose, 121.25 ± 11.03 mg/dL) and diabetic db/db mice (C57BLKs; body weight, 46.94 ± 1.52 g; blood glucose, 225.0 ± 19.32 mg/dL) (n = 5), db/db mice were injected with the scramble or miR-539-5p mimics at a dose of 5 mg/kg body weight i.v. via the tail vein using *in vivo*-jetPEI (three doses, one every other day). db/+ animals were injected with a scramble oligonucleotide. One day after the last injection, animals were fasted overnight, and an OGTT was performed as described below. Animals were then euthanized, and blood and skeletal muscle tissue were collected and stored for metabolic profiling and qRT-PCR as described. *In-vivo*-injected oligonucleotides had 2′O-methyl modifications with phosphorothioate linkages and a cholesterol moiety linked at the 3′ end by a hydroxyprolinol linkage (Sigma, MO, USA). All animal experiments were approved by the Institute Animal Ethical Committee and regulated by the Committee for the Purpose of Control and Supervision of Experiments on Animals (CPCSEA) (New Delhi, India).

DNMT activity assay

DNMT activity in skeletal muscle of normal and diabetic mice or cell lysates was measured using the colorimetric DNMT activity quantification kit (Abcam, UK) according to the manufacturer's instructions. Briefly, 20 μg of lysate (lysed in RIPA lysis buffer containing protease and phosphatase inhibitor) was incubated with Adomet buffer (containing S-adenosyl methionine) in a universal DNMT substrate-coated microplate, and the methylated DNA (substrate) was quantified using a capture antibody (anti-5-methycytosine antibody) and a detection antibody. Absorbance was measured in a microplate reader (Tecan, Switzerland) at 450 nm, and DNMT activity was expressed as optical density (OD) per hour per microgram of protein.

Cell culture and treatment

C2C12, mouse myoblast, and mouse Hepa1-6 cells were obtained from the National Centre for Cell Science (NCCS) (Pune, India) and maintained in high-glucose Dulbecco's modified Eagle's medium (DMEM) supplemented with 10% (v/v) fetal bovine serum (Gibco, Cambridge, UK) and antibiotic/antimycotic solution (Gibco) at 37°C in 5% CO_2. At a confluence of 70%–80%, the medium of C2C12 cells was replaced with high-glucose DMEM supplemented with 2% (v/v) horse serum (Gibco), to promote differentiation of myoblasts into myotubes, which were visible within 4 days of incubation. Differentiated cells were transfected with the scramble or mimics of miR-539-5p, miR381-3p, or miR-31-5p (1–50 nM) (Dharmacon). Wherever mentioned, along with the miR-539-5p mimic, the scramble or the miR-539-5p inhibitor (Dharmacon) was co-transfected at a concentration of 50 nM using Lipofectamine RNAimax (Invitrogen, MA, USA) and OptiMEM (Gibco). After 48 h of incubation, cells were harvested for qRT-PCR and western blotting to evaluate target gene expression. For the miR-539-5p inhibitor studies, C2C12 cells transfected with the scramble or miR-539-5p inhibitor (25–50nM) were harvested after 48 h to evaluate the levels of DNMT3b and *Srebf1*. For validation in primary cells, human primary myoblast cells (PromoCell, Germany) were cultured in 12-well plates (CellBIND, Corning, NY, USA) in skeletal muscle growth medium (PromoCell) according to the manufacturer's instructions. Upon attaining 80% confluence, cells were transfected as above and harvested for further use. For *Dnmt3b* siRNA treatment, differentiated C2C12 cells were transfected with the scramble or *Dnmt3b* siRNA (50–100 nM) (Sigma) using Lipofectamine RNAimax (Invitrogen) and OptiMEM (Gibco); upon termination of incubation at 48 h, cells were harvested for qRT-PCR and western blotting as described below. To confirm the effects of DNMT3b inhibition, differentiated C2C12 cells were incubated in the presence of DMSO or the DNMT3b inhibitor NA (Calbiochem, MA, USA) at a dose of 1, 5, and 10 μM as described by Lai et al.[28] After 48 h, cells were harvested, lysed, and processed as described below to evaluate *Dnmt1*, *Dnmt3a*, *Dnmt3b*, and *Srebf1* levels. Whether DNMT3b mediates the effects of miR-539-5p on *Srebf1* was studied by co-transfecting C2C12 cells with the miR-539-5p inhibitor (50 nM) with the scramble or *Dnmt3b* siRNA (100 nM), and after 48 h, *Dnmt3b* and *Srebf1* transcript levels were evaluated by qRT-PCR as described below. To explore the effect of overexpression of miR-539-5p in the liver, mouse hepatic Hepa 1-6 cells were transfected with the scramble or miR-539-5p mimic (50 nM). After 48 h of incubation, cells were harvested to evaluate the expression of miR-539-5p, *Dnmt3b*, and *Srebf1*.

RNA isolation and qRT-PCR

RNA from cells and tissues was isolated using TRIzol according to the manufacturer's protocol and quantified using a plate reader (Infinite 200 Pro, Tecan, Switzerland) with 260/280 ratios between 1.9 and 2.0. 1 μg of RNA was used for cDNA synthesis using RevertAid reverse transcriptase (Thermo Fisher Scientific, USA) and random hexamers (Thermo Fisher Scientific, MA, USA). Quantitative PCR was performed to evaluate gene and miRNA expression in a StepOne Plus real-time PCR machine (Applied Biosystems, MA, USA) using SYBR Green Master Mix (Applied Biosystems, USA) and primers as in Table S1. 18S rRNA and Sno234 were used as normalization controls for genes and miRNA expression, respectively. Relative gene expression was calculated by the ΔCt method.[55]

Western blotting

Protein samples were isolated from cells and tissues using RIPA lysis buffer (Sigma) containing phosphatase (Calbiochem, Germany) and protease inhibitors (Calbiochem, Germany). 40 μg of protein was run on SDS-PAGE and subjected to western blot analysis using DNMT1 (Cell Signaling Technology, MA, USA; 1:2,000 dilution), DNMT3a (Cell Signaling Technology, MA, USA; 1:2,000 dilution), and DNMT3b (Abcam, UK; 1:2,000 dilution) antibodies. Immunoreactive bands were detected using horseradish peroxidase (HRP)-linked secondary antibodies (Genei, India), followed by detection with femtoLUCENT HRP-Plus reagent (G-Bioscience, MO, USA). HSC70 was used as the loading control for normalization. Densiometric analyses for western blots were performed using AlphaEase FC imaging analysis software (Alpha Innotech, CA, USA), and the intensity of each band was normalized to background intensity.

Cloning, mutagenesis, and luciferase assay

Luciferase reporter constructs containing the 3′ UTR of *Dnmt3b* harboring the binding site for miR-539-5p were generated in a psiCheck2 vector (Promega, WI, USA) using primers as in Table S1. Substitution mutation was done in the binding site of miR-539-5p using the XL site-directed mutagenesis kit (Agilent Technologies, Canada) and mutation-specific primers (Table S1). Differentiated C2C12 cells were co-transfected with the WT (100 ng) or the MT 3′ UTR reporter plasmid (100 ng) along with the scramble or the miR-539-5p mimic (50 nM) with or without the miR-539-5p inhibitor (50 nM). A dual luciferase assay (Promega, USA) was performed after 48 h of incubation, and luminescence was measured in a multimode reader (Infinite M200 Pro, Tecan, Switzerland). *Renilla* luciferase values were normalized to those of firefly luciferase. As described by Phatak and Donahue,[56] to validate the binding of miR-539-5p with the 3′ UTR of *Dnmt3b* mRNA, C2C12 cells were transfected with biotin-labeled scramble or biotin-labeled miR-539-5p mimic (50 nM) (QIAGEN, USA). After 48 h of incubation, cells were harvested, lysed, and incubated overnight with Dynabead-linked

Streptavidin C1 (Thermo Fisher Scientific, USA) at 4°C. Dynabeads were pulled down on a magnetic stand, and the bound RNA was isolated by using TRIzol. Enrichment of *Dnmt3b* mRNA with biotin-labeled miR-539-5p mimic was quantified by real-time PCR using *Dnmt3b*-specific primers and compared with that of scramble-transfected cells.

The complete coding sequence of mouse *Dnmt3b* was cloned into a pcDNA3.1(+) vector (Thermo Fisher Scientific, USA) using specific primers (Table S1). Differentiated C2C12 cells were transfected with the empty vector or the *Dnmt3b* overexpression vector (0.5–1 μg) alone or with the miR-539-5p mimic (50 nM) using Lipofectamine 2000 (Invitrogen, USA) according to the manufacturer's protocol. After 48 h, cells were lysed, total RNA was isolated, and the transcript levels of *Srebf1* were assessed by qRT-PCR as described above.

Bioinformatics analysis

miRNA target prediction was performed using three online public databases: TargetScan (http://www.targetscan.org/vert_72/), mirDB (http://mirdb.org/mirdb/index.html), and miRanda (http://microrna.org/). The presence of CpG islands within the genes was analyzed using the UCSC Genome Browser (https://genome.ucsc.edu/).

MeDIP

Differentiated C2C12 cells were transfected with scramble (50 nM) or miR-539-5p mimic (50 nM) for 48 h. Upon termination of incubation, genomic DNA was isolated from these cells and from skeletal muscle of db/+ and db/db animals using phenol/chloroform/isoamyl alcohol. Isolated genomic DNA was randomly sheared into 200- to 700-bp fragments with six sets of sonication cycles (15-s pulse and 30-s incubation between each pulse) using an ultrasonic homogenizer (Takashi, Japan). Sonicated genomic DNA was quantified in a plate reader (Infinite 200 Pro, Tecan, Switzerland); 2 μg of sonicated genomic DNA was used for immunoprecipitation with 5-methylcytosine antibody (2 μg) (Epigentek, USA) or non-immune rabbit immunoglobulin G (IgG) (Epigentek, USA) and incubated overnight at 4°C. Methylation-enriched CpG regions within the *Srebf1* gene were quantified by real-time PCR using CpG region-specific primers (primers against each CpG island split into regions of 150–180 bp; Table S1).

OGTT

Scramble- and miR-539-5p antagomir-injected mice or db/+ and db/db mice were fasted for 12 h for an OGTT. Fasting blood glucose was measured prior to an oral glucose dose (2 g/kg body weight) for the OGTT. Blood glucose levels were measured at time intervals of 30, 60, 90, and 120 min after the oral glucose feed.

Blood and tissue collection

Blood glucose was measured using the OneTouch Select glucometer (Life Scan Europe, Switzerland). For insulin, cholesterol, and triglyceride analysis, blood samples were collected from mice during euthanization, centrifuged at 1,300 × *g* for 10 min at 4°C to collect serum, and stored at −20°C for further use. Insulin levels were measured using the insulin ELISA kit (G-Biosciences, USA) according to the manufacturer's protocol. Serum triglycerides, cholesterol, and cholesteryl ester levels were measured using the respective kits following the manufacturer's instructions (BioVision, CA, USA). Skeletal muscle was isolated from all groups of mice and stored in RNAlater (Ambion, USA) at −80°C or directly transferred to −80°C for protein analysis.

Statistical analysis

All experiments were performed at least three times, and data are represented as means ± SEM. Student's t test and one-way ANOVA were performed for statistical significance; $p < 0.05$ was considered statistically significant.

Data availability

The datasets generated and/or analyzed during the current study are available from the corresponding author upon reasonable request.

SUPPLEMENTAL INFORMATION

Supplemental information can be found online at https://doi.org/10.1016/j.omtn.2022.08.013.

ACKNOWLEDGMENTS

We thank Mayank Garg and Rukshar Khan for help with the experiments and Dr. Shagun Poddar for help with standardizing cell culture experiments. This work was supported by funding from the Council of Scientific & Industrial Research (CSIR), New Delhi, India (BSC0122 and MLP2013). D.K., A.K., and A.R. acknowledge the Council of Scientific and Industrial Research for their fellowships.

AUTHOR CONTRIBUTIONS

M.D. conceived and designed the experiments. D.K. standardized and performed most of the experiments. A.K. performed the cloning experiment to assess the rescue of the miRNA effect. A.R. performed the nanaomycin A experiments. D.K. and M.D. analyzed the data and wrote the paper. All authors read and approved the final manuscript.

DECLARATION OF INTEREST

The authors declare no competing interests.

REFERENCES

1. Cole, J.B., and Florez, J.C. (2020). Genetics of diabetes mellitus and diabetes complications. Nat. Rev. Nephrol. *16*, 377–390.

2. Murea, M., Ma, L., and Freedman, B.I. (2012). Genetic and environmental factors associated with type 2 diabetes and diabetic vascular complications. Rev. Diabet. Stud. *9*, 6–22.

3. Ling, C., and Groop, L. (2009). Epigenetics: a molecular link between environmental factors and type 2 diabetes. Diabetes *58*, 2718–2725.

4. Zhao, J., Goldberg, J., Bremner, J.D., and Vaccarino, V. (2012). Global DNA methylation is associated with insulin resistance. Diabetes *61*, 542–546.

5. Moore, L.D., Le, T., and Fan, G. (2013). DNA methylation and its basic function. Neuropsychopharmacology *381*, 23–38.

6. Barrès, R., Yan, J., Egan, B., Treebak, J.T., Rasmussen, M., Fritz, T., Caidahl, K., Krook, A., O'Gorman, D.J., and Zierath, J.R. (2012). Acute exercise remodels promoter methylation in human skeletal muscle. Cell Metab. *15*, 405–411.

7. Barres, R., Kirchner, H., Rasmussen, M., Yan, J., Kantor, F.R., Krook, A., Näslund, E., and Zierath, J.R. (2013). Weight loss after gastric bypass surgery in human obesity remodels promoter methylation. Cell Rep. *3*, 1020–1027.

8. Jinawath, A., Miyake, S., Yanagisawa, Y., Akiyama, Y., and Yuasa, Y. (2005). Transcriptional regulation of the human DNA methyltransferase 3A and 3B genes by Sp3 and Sp1 zinc finger proteins. Biochem. J. *385*, 557–564.

9. Peterson, E.J., Bögler, O., and Taylor, S.M. (2003). p53-Mediated repression of DNA methyltransferase 1 expression by specific DNA binding 1. Cancer Res. *63*, 6579–6582.

10. Kimura, H., Nakamura, T., Ogawa, T., Tanaka, S., and Shiota, K. (2003). Transcription of mouse DNA methyltransferase 1 (Dnmt1) is regulated by both E2F-Rb-HDAC-dependent and -independent pathways. Nucleic Acids Res. *31*, 3101–3113.

11. Yang, Y.C., Tang, Y.A., Shieh, J.M., Lin, R.K., Hsu, H.S., and Wang, Y.C. (2014). DNMT3B overexpression by deregulation of FOXO3a-mediated transcription repression and MDM2 overexpression in lung cancer. J. Thorac. Oncol. *9*, 1305–1315.

12. Ling, Y., Sankpal, U.T., Robertson, A.K., McNally, J.G., Karpova, T., and Robertson, K.D. (2004). Modification of de novo DNA methyltransferase 3a (Dnmt3a) by SUMO-1 modulates its interaction with histone deacetylases (HDACs) and its capacity to repress transcription. Nucleic Acids Res. *32*, 598–610.

13. Wang, J., Hevi, S., Kurash, J.K., Lei, H., Gay, F., Bajko, J., Su, H., Sun, W., Chang, H., Xu, G., et al. (2008). The lysine demethylase LSD1 (KDM1) is required for maintenance of global DNA methylation. Nat. Genet. *41*, 125–129.

14. Estève, P.O., Chang, Y., Samaranayake, M., Upadhyay, A.K., Horton, J.R., Feehery, G.R., Cheng, X., and Pradhan, S. (2010). A methylation and phosphorylation switch between an adjacent lysine and serine determines human DNMT1 stability. Nat. Struct. Mol. Biol. *18*, 42–48.

15. Goyal, R., Rathert, P., Laser, H., Gowher, H., and Jeltsch, A. (2007). Phosphorylation of serine-515 activates the mammalian maintenance methyltransferase Dnmt1. Epigenetics *2*, 155–160.

16. López de Silanes, I., Gorospe, M., Taniguchi, H., Abdelmohsen, K., Srikantan, S., Alaminos, M., Berdasco, M., Urdinguio, R.G., Fraga, M.F., Jacinto, F.V., and Esteller, M. (2009). The RNA-binding protein HuR regulates DNA methylation through stabilization of DNMT3b mRNA. Nucleic Acids Res. *37*, 2658–2671.

17. Fabbri, M., Garzon, R., Cimmino, A., Liu, Z., Zanesi, N., Callegari, E., Liu, S., Alder, H., Costinean, S., Fernandez-Cymering, C., et al. (2007). MicroRNA-29 family reverts aberrant methylation in lung cancer by targeting DNA methyltransferases 3A and 3B. Proc. Natl. Acad. Sci. USA *104*, 15805–15810.

18. Garzon, R., Liu, S., Fabbri, M., Liu, Z., Heaphy, C.E.A., Callegari, E., Schwind, S., Pang, J., Yu, J., Muthusamy, N., et al. (2009). MicroRNA-29b induces global DNA hypomethylation and tumor suppressor gene reexpression in acute myeloid leukemia by targeting directly DNMT3A and 3B and indirectly DNMT1. Blood *113*, 6411–6418.

19. Duursma, A.M., Kedde, M., Schrier, M., le Sage, C., and Agami, R. (2008). miR-148 targets human DNMT3b protein coding region. RNA *14*, 872–877.

20. Braconi, C., Huang, N., and Patel, T. (2010). MicroRNA-dependent regulation of DNA methyltransferase-1 and tumor suppressor gene expression by interleukin-6 in human malignant cholangiocytes. Hepatology *51*, 881–890.

21. Liu, R., Gu, J., Jiang, P., Zheng, Y., Liu, X., Jiang, X., Huang, E., Xiong, S., Xu, F., Liu, G., et al. (2015). Biology of human tumors DNMT1-MicroRNA126 epigenetic circuit contributes to esophageal squamous cell carcinoma growth via ADAM9-EGFR-AKT signaling. Clin. Cancer Res. *21*, 854–863.

22. Barrès, R., Osler, M.E., Yan, J., Rune, A., Fritz, T., Caidahl, K., Krook, A., and Zierath, J.R. (2009). Non-CpG methylation of the PGC-1α promoter through DNMT3B controls mitochondrial density. Cell Metab. *10*, 189–198.

23. Jacobsen, S.C., Brøns, C., Bork-Jensen, J., Ribel-Madsen, R., Yang, B., Lara, E., Hall, E., Calvanese, V., Nilsson, E., Jørgensen, S.W., et al. (2012). Effects of short-term high-fat overfeeding on genome-wide DNA methylation in the skeletal muscle of healthy young men. Diabetologia *55*, 3341–3349.

24. Nitert, M.D., Dayeh, T., Volkov, P., Elgzyri, T., Hall, E., Nilsson, E., Yang, B.T., Lang, S., Parikh, H., Wessman, Y., et al. (2012). Impact of an exercise intervention on DNA methylation in skeletal muscle from first-degree relatives of patients with type 2 diabetes. Diabetes *61*, 3322–3332.

25. Ribel-Madsen, R., Fraga, M.F., Jacobsen, S., Bork-Jensen, J., Lara, E., Calvanese, V., Fernandez, A.F., Friedrichsen, M., Vind, B.F., Højlund, K., et al. (2012). Genome-wide analysis of DNA methylation differences in muscle and fat from monozygotic twins discordant for type 2 diabetes. PLoS One *7*, e51302.

26. Agarwal, P., Srivastava, R., Srivastava, A.K., Ali, S., and Datta, M. (2013). miR-135a targets IRS2 and regulates insulin signaling and glucose uptake in the diabetic gastrocnemius skeletal muscle. Biochim. Biophys. Acta *1832*, 1294–1303.

27. Kesharwani, D., Kumar, A., Poojary, M., Scaria, V., and Datta, M. (2021). RNA sequencing reveals potential interacting networks between the altered transcriptome and ncRNome in the skeletal muscle of diabetic mice. Biosci. Rep. *41*, 20210495.

28. Lai, S.C., Su, Y.T., Chi, C.C., Kuo, Y.C., Lee, K.F., Wu, Y.C., et al. (2019). DNMT3b/OCT4 expression confers sorafenib resistance and poor prognosis of hepatocellular carcinoma through IL-6/STAT3 regulation. J. Exp. Clin. Cancer Res. *38*, 474–491.

29. Kuck, D., Caulfield, T., Lyko, F., and Medina-Franco, J.L. (2010). Nanaomycin A selectively inhibits DNMT3B and reactivates silenced tumor suppressor genes in human cancer cells. Mol. Cancer Ther. *9*, 3015–3023.

30. Zhang, P., Zhao, M., Liang, G., Yin, G., Huang, D., Su, F., Zhai, H., Wang, L., Su, Y., and Lu, Q. (2013). Whole-genome DNA methylation in skin lesions from patients with psoriasis vulgaris. J. Autoimmun. *41*, 17–24.

31. Ligthart, S., Marzi, C., Aslibekyan, S., Mendelson, M.M., Conneely, K.N., Tanaka, T., et al. (2016). DNA methylation signatures of chronic low-grade inflammation are associated with complex diseases. Genome Biol. *17*, 255–269.

32. Serra-Juhé, C., Cuscó, I., Homs, A., Flores, R., Torán, N., and Pérez-Jurado, L.A. (2015). DNA methylation abnormalities in congenital heart disease. Epigenetics *10*, 167–177.

33. Kulis, M., and Esteller, M. (2010). DNA methylation and cancer. Adv. Genet. *70*, 27–56.

34. Qin, W., Leonhardt, H., and Pichler, G. (2011). Regulation of DNA methyltransferase 1 by interactions and modifications. Nucleus *2*, 392–402.

35. Aravin, A.A., Sachidanandam, R., Bourc'his, D., Schaefer, C., Pezic, D., Toth, K.F., Bestor, T., and Hannon, G.J. (2008). A piRNA pathway primed by individual transposons is linked to de novo DNA methylation in mice. Mol. Cell *31*, 785–799.

36. Denis, H., Ndlovu, 'M.N, and Fuks, F. (2011). Regulation of mammalian DNA methyltransferases: a route to new mechanisms. EMBO Rep. *12*, 647–656.

37. Sinkkonen, L., Hugenschmidt, T., Berninger, P., Gaidatzis, D., Mohn, F., Artus-Revel, C.G., Zavolan, M., Svoboda, P., and Filipowicz, W. (2008). MicroRNAs control de novo DNA methylation through regulation of transcriptional repressors in mouse embryonic stem cells. Nat. Struct. Mol. Biol. *15*, 259–267.

38. Benetti, R., Gonzalo, S., Jaco, I., Muñoz, P., Gonzalez, S., Schoeftner, S., Murchison, E., Andl, T., Chen, T., Klatt, P., et al. (2008). A mammalian microRNA cluster controls DNA methylation and telomere recombination via Rbl2-dependent regulation of DNA methyltransferases. Nat. Struct. Mol. Biol. *15*, 998.

39. Nowialis, P., Lopusna, K., Opavska, J., Haney, S.L., Abraham, A., Sheng, P., et al. (2019). Catalytically inactive Dnmt3b rescues mouse embryonic development by accessory and repressive functions. Nat. Commun. *10*, 4374–4389.

40. Lopusna, K., Nowialis, P., Opavska, J., Abraham, A., Riva, A., and Opavsky, R. (2021). Dnmt3b catalytic activity is critical for its tumour suppressor function in lymphomagenesis and is associated with c-Met oncogenic signalling. EBioMedicine *63*, 103191.

41. Shimomura, I., Shimano, H., Horton, J.D., Goldstein, J.L., and Brown, M.S. (1997). Differential expression of exons 1a and 1c in mRNAs for sterol regulatory element binding protein-1 in human and mouse organs and cultured cells. J. Clin. Invest. *99*, 838–845.

42. Shimano, H., Amemiya-Kudo, M., Takahashi, A., Kato, T., Ishikawa, M., and Yamada, N. (2007). Sterol regulatory element–binding protein-1c and pancreatic β-cell dysfunction. Diabetes, Obes. Metab. *9*, 133–139.

43. Lin, Y., Ding, D., Huang, Q., Liu, Q., Lu, H., Lu, Y., Chi, Y., Sun, X., Ye, G., Zhu, H., et al. (2017). Downregulation of miR-192 causes hepatic steatosis and lipid accumulation by inducing SREBF1: novel mechanism for bisphenol A-triggered non-alcoholic fatty liver disease. Biochim. Biophys. Acta. Mol. Cell Biol. Lipids *1862*, 869–882.

44. You, Z., Li, B., Xu, J., Chen, L., and Ye, H. (2018). Curcumin suppress the growth of hepatocellular carcinoma via down-regulating SREBF1. Oncol. Res.

45. Ivatt, R.M., and Whitworth, A.J. (2014). SREBF1 links lipogenesis to mitophagy and sporadic Parkinson disease. Autophagy *10*, 1476–1477.

46. Eberlé, D., Clément, K., Meyre, D., Sahbatou, M., Vaxillaire, M., Le Gall, A., Ferré, P., Basdevant, A., Froguel, P., and Foufelle, F. (2004). SREBF-1 gene polymorphisms are associated with obesity and type 2 diabetes in French obese and diabetic cohorts. Diabetes *53*, 2153–2157.

47. Demenais, F., Kanninen, T., Lindgren, C.M., Wiltshire, S., Gaget, S., Dandrieux, C., Almgren, P., Sjögren, M., Hattersley, A., Dina, C., et al. (2003). A meta-analysis of four European genome screens (GIFT Consortium) shows evidence for a novel region on chromosome 17p11.2–q22 linked to type 2 diabetes. Hum. Mol. Genet. *12*, 1865–1873.

48. Laudes, M., Barroso, I., Luan, J., Soos, M.A., Yeo, G., Meirhaeghe, A., Logie, L., Vidal-Puig, A., Schafer, A.J., Wareham, N.J., and O'Rahilly, S. (2004). Genetic variants in human sterol regulatory element binding protein-1c in syndromes of severe insulin resistance and type 2 diabetes. Diabetes *53*, 842–846.

49. Grarup, N., Stender-Petersen, K.L., Andersson, E.A., Jørgensen, T., Borch-Johnsen, K., Sandbæk, A., Lauritzen, T., Schmitz, O., Hansen, T., and Pedersen, O. (2008). Association of variants in the sterol regulatory element-binding factor 1 (SREBF1) gene with type 2 diabetes, glycemia, and insulin resistance. Diabetes *57*, 1136–1142.

50. Ide, T., Shimano, H., Yahagi, N., Matsuzaka, T., Nakakuki, M., Yamamoto, T., Nakagawa, Y., Takahashi, A., Suzuki, H., Sone, H., et al. (2004). SREBPs suppress IRS-2-mediated insulin signalling in the liver. Nat. Cell Biol. *6*, 351–357.

51. Horton, J.D., Goldstein, J.L., and Brown, M.S. (2002). SREBPs: activators of the complete program of cholesterol and fatty acid synthesis in the liver. J. Clin. Invest. *109*, 1125–1131.

52. Guillet-Deniau, I., Mieulet, V., Le Lay, S., Achouri, Y., Carré, D., Girard, J., Foufelle, F., and Ferré, P. (2002). Sterol regulatory element binding protein-1c expression and action in rat muscles: insulin-like effects on the control of glycolytic and lipogenic enzymes and UCP3 gene expression. Diabetes *51*, 1722–1728.

53. Sewter, C., Berger, D., Considine, R.V., Medina, G., Rochford, J., Ciaraldi, T., Henry, R., Dohm, L., Flier, J.S., O'Rahilly, S., and Vidal-Puig, A.J. (2002). Human obesity and type 2 diabetes are associated with alterations in SREBP1 isoform expression that are reproduced ex vivo by tumor necrosis factor-α. Diabetes *51*, 1035–1041.

54. Krause, C., Sievert, H., Geißler, C., Grohs, M., El Gammal, A.T., Wolter, S., Ohlei, O., Kilpert, F., Krämer, U.M., Kasten, M., et al. (2019). Critical evaluation of the DNA-methylation markers ABCG1 and SREBF1 for Type 2 diabetes stratification. Epigenomics *11*, 885–897.

55. Pfaffl, M.W. (2001). A new mathematical model for relative quantification in real-time RT–PCR. Nucleic Acids Res. *29*, e45.

56. Phatak, P., and Donahue, J.M. (2017). Biotinylated micro-RNA pull down assay for identifying miRNA targets. Bio. Protoc. *7*, e2253.